

CORRECTION NOTICE

Nat. Neurosci. 14, 387–397 (2011)

An optogenetic toolbox designed for primates

Ilka Diester, Matthew T Kaufman, Murtaza Mogri, Ramin Pashaie, Werapong Goo, Ofer Yizhar, Charu Ramakrishnan, Karl Deisseroth & Krishna V Shenoy

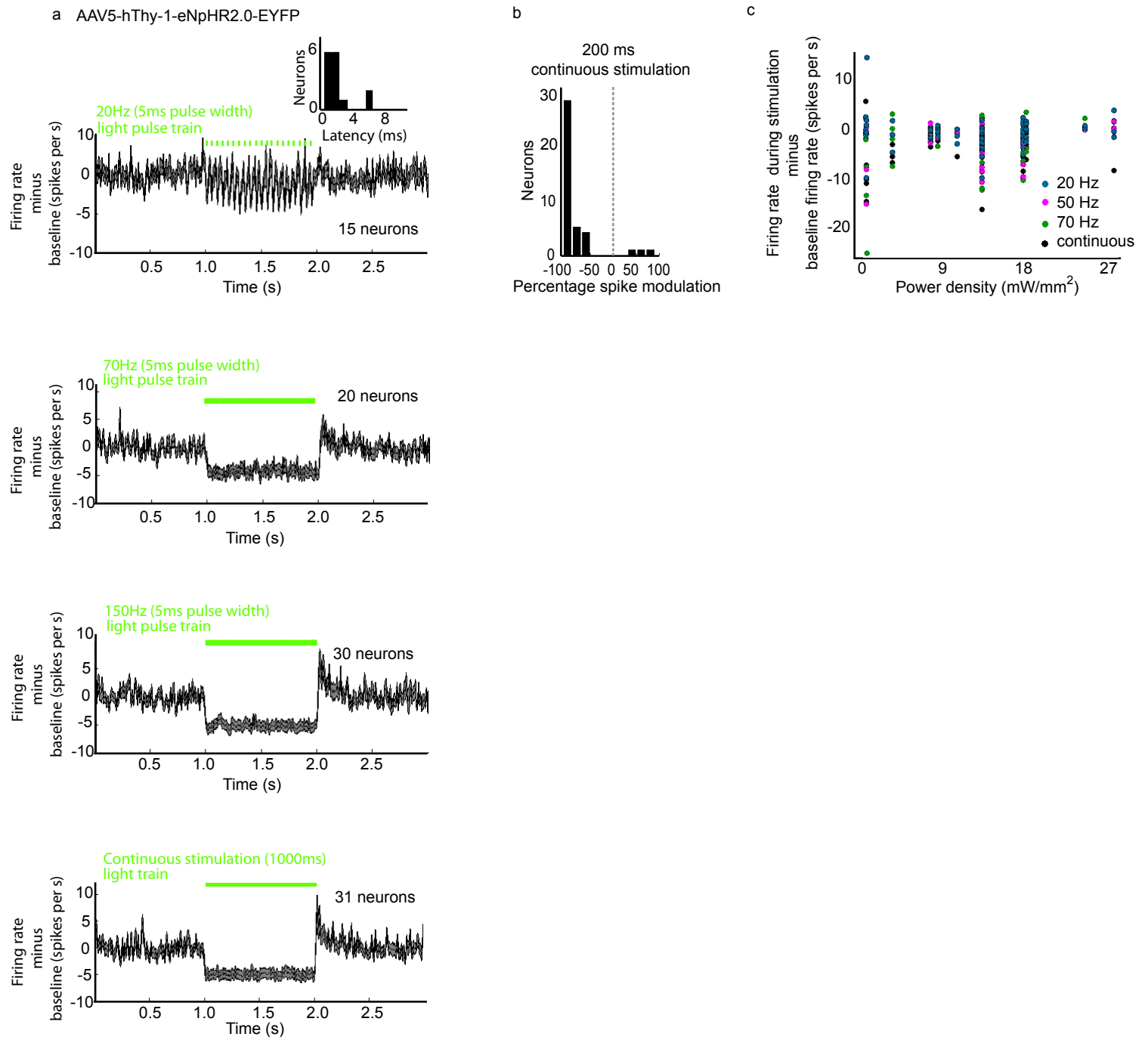
In the version of this supplementary file originally posted online, two tables were missing. The error has been corrected in this file as of 25 February 2011.

SUPPLEMENTARY MATERIAL

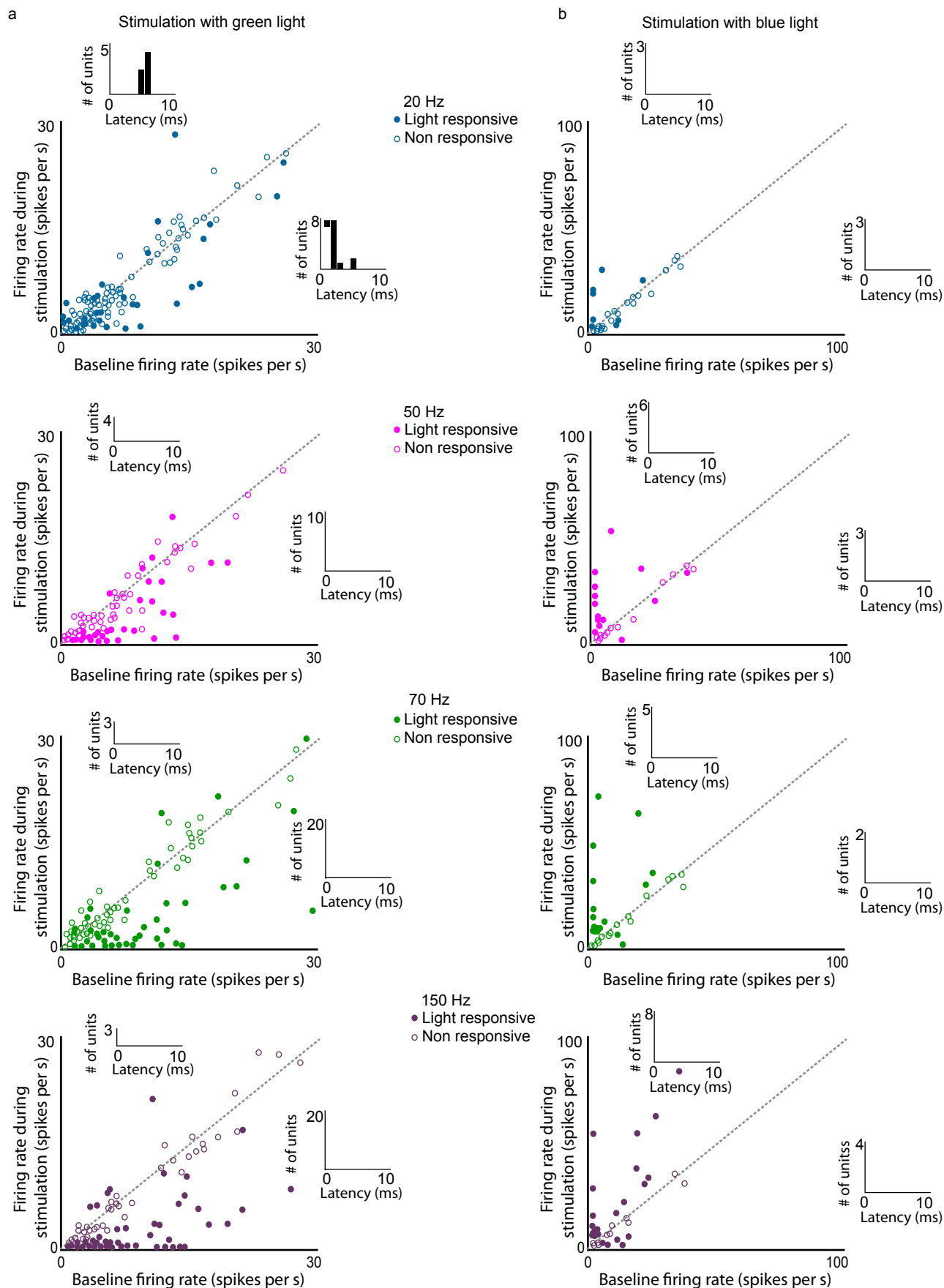
An Optogenetic Toolbox Designed for Primates

Ilka Diester, Matthew T. Kaufman, Murtaza Mogri,
Ramin Pashaie, Werapong Goo, Ofer Yizhar, Charu Ramakrishnan,
Karl Deisseroth, Krishna V. Shenoy

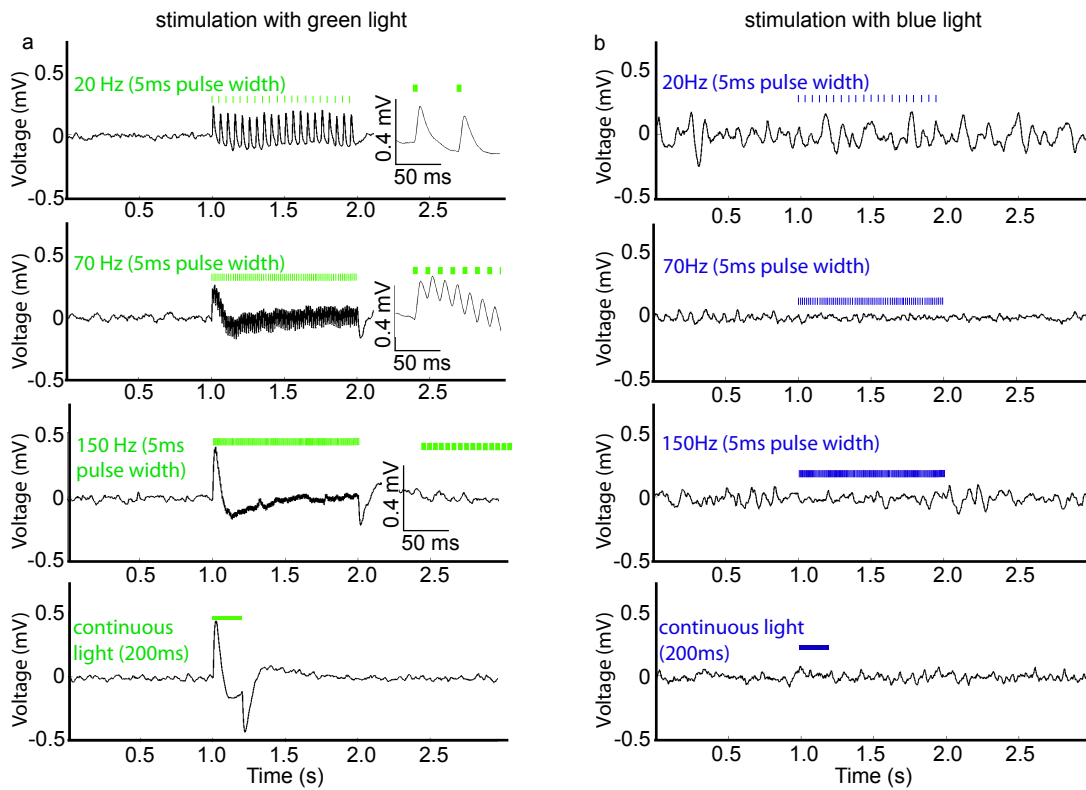
Correspondence should be addressed to
K.S. (shenoy@stanford.edu) or K.D. (deissero@stanford.edu)



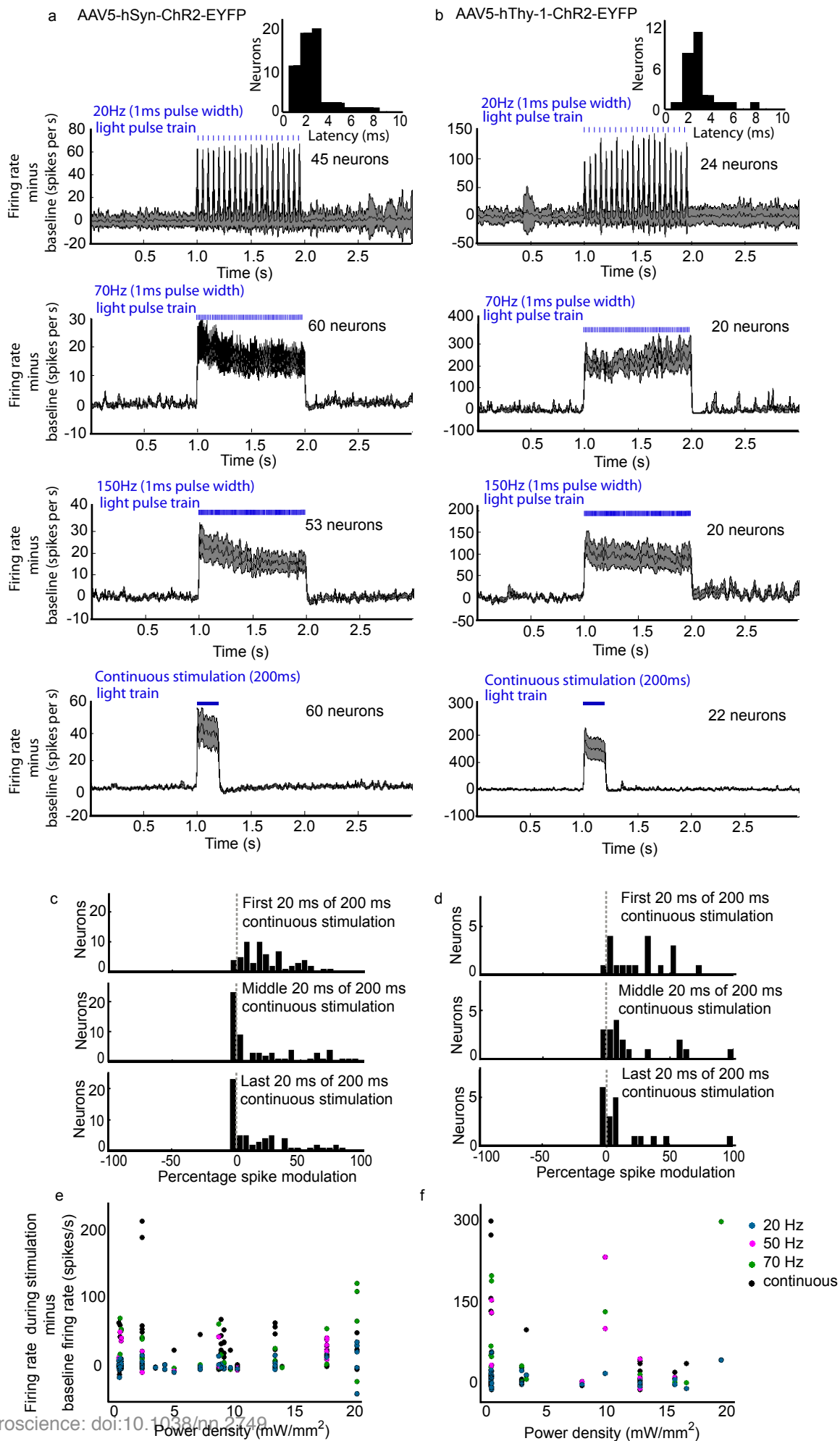
Supplementary Figure 1. Average neuronal population responses to light, spike modulation, and applied light intensities at the eNpHR2.0 expressing site. **(a)** Population PSTHs (baseline subtracted average \pm SEM) of significantly modulated neurons during optical stimulation. Inset in 20 Hz panel shows the latency distribution measured during 20 Hz stimulation of significantly light responsive neurons. **(b)** Spike modulations of significantly light-responsive neurons measured during 200 ms continuous stimulation for neurons. **(c)** Applied light intensities. The differences between baseline firing rate and firing rate during optical stimulation are plotted against the applied power densities. Each dot represents a neuron-stimulation protocol combination. Different colors represent different stimulation parameters: blue - 20Hz, magenta - 50 Hz, green - 70 Hz, black - continuous stimulation. Power densities causing neural modulation at the recording sites ranged from 0.34 mW/mm^2 to 27 mW/mm^2 .



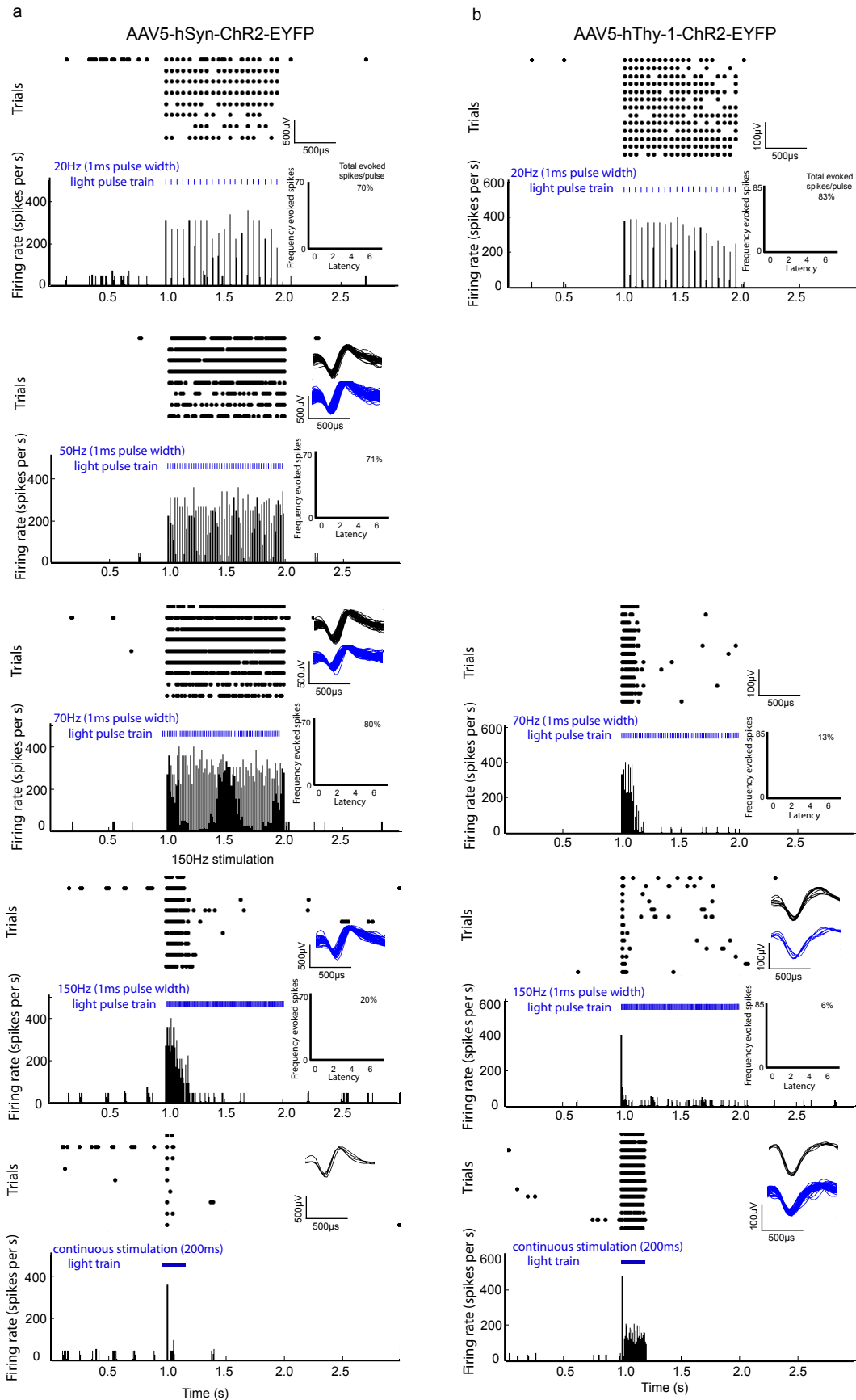
Supplementary Figure 2. Firing rate modulation of single and multi units caused by green and blue light recorded at an eNpHR2.0 expressing site. **(a)** Responses and latencies during green light stimulation. Firing rates during stimulation are plotted against baseline firing rates (without stimulation). Empty circles show non-significant responses to light, filled circles show significant responses. Note that not all units were tested with the full set of frequencies. The dashed gray line is the unity-slope line. Insets depict latency distribution of units which responded with an increase of their firing rate during stimulation (dots above the gray dashed line) or with a decrease of their firing rate during stimulation (dots beneath the gray dashed line). **(b)** Responses and latencies during blue light stimulation. Same layout as in a.



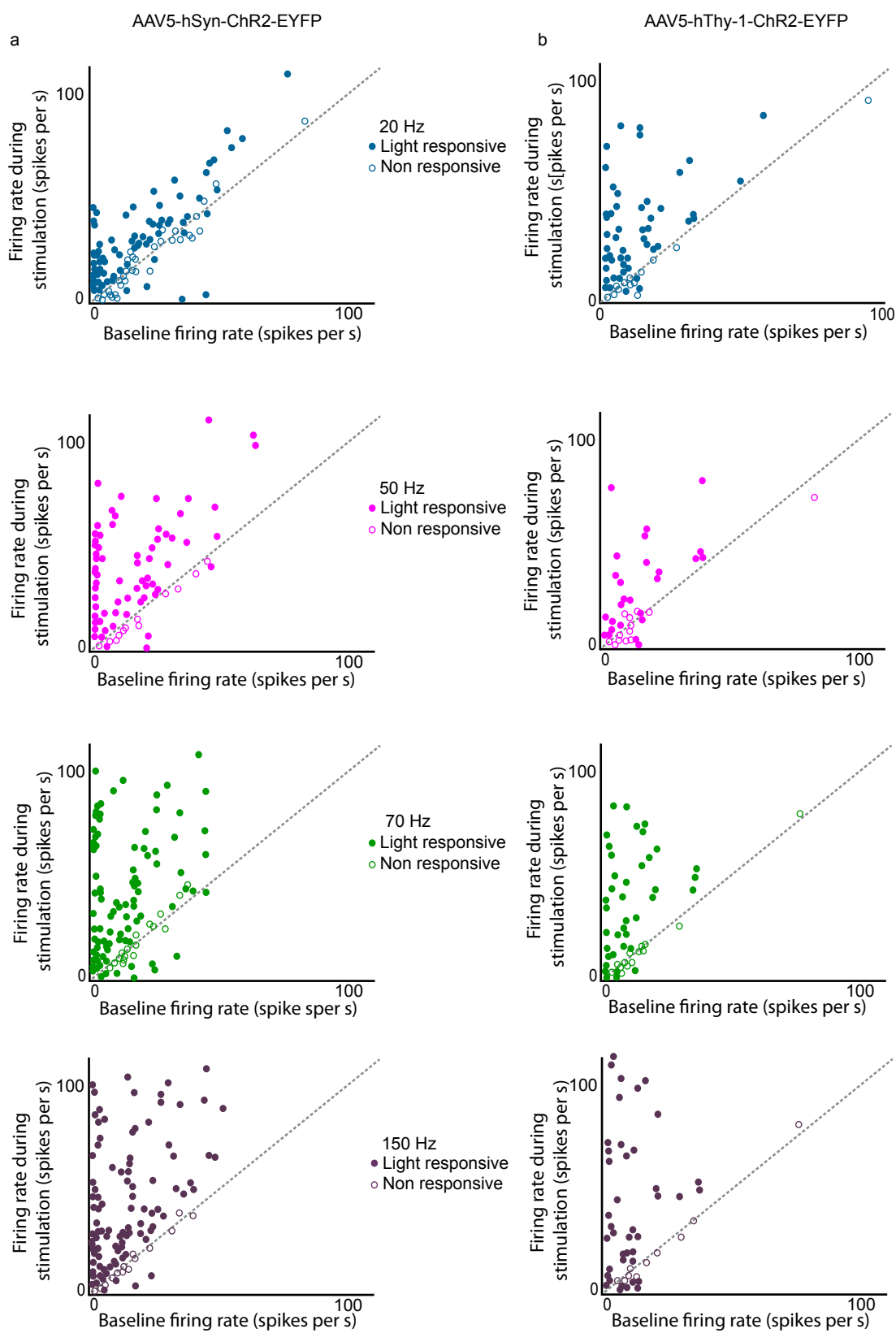
Supplementary Figure 4. Local field potential deflections in eNpHR2.0-expressing regions during optical stimulation. **(a)** Local field potential deflections (averaged across 5 to 10 trials) in response to green light with increasing frequencies from top to bottom (20, 70, 150 Hz and 200 ms continuous stimulation). Deflections are positive and show a negative rebound effect after the end of stimulation (particularly obvious for 200 ms continuous light). The direction of the deflection is as expected based on the ion flow: Cl^- is pumped into neurons, causing a relative increase of positive charges (positive deflections of the LFP signal) in the extracellular milieu. Insets depict an expanded view of the averaged LFP traces. **(b)** Measurements during blue light stimulation at the same area as in a. No prominent LFP deflections are visible.



Supplementary Figure 5. Average neuronal population responses to light and spike modulation. **(a,b)** Population PSTHs (baseline subtracted average \pm SEM) of significantly modulated neurons during optical stimulation. Inset in 20 Hz panel shows the latency distribution measured during 20 Hz stimulation of significantly light responsive neurons. **(a)** AAV5-hSyn-ChR2-EYFP, **(b)** AAV5-hThy-1-ChR2-EYFP. **(c,d)** Spike modulations of significantly light-responsive neurons measured during 200 ms continuous stimulation for neurons. **(c)** AAV5-hSyn-ChR2-EYFP, **(d)** AAV5-hThy-1-ChR2-EYFP. Separate distributions are plotted for the first, middle, and last 20 ms following light onset to show the dynamic response properties. **(e,f)** Applied light intensities. The differences between baseline firing rate and firing rate during optical stimulation are plotted against the applied power densities. Each dot represents a neuron-stimulation protocol combination. Different colors represent different stimulation parameters: blue - 20Hz, magenta - 50 Hz, green - 70 Hz, black - continuous stimulation. Power densities causing neural modulation at the recording sites ranged from 0.25 mW/mm² to 20 mW/mm². **(e)** AAV5-hSyn-ChR2-EYFP, **(f)** AAV5-hThy-1-ChR2-EYFP.

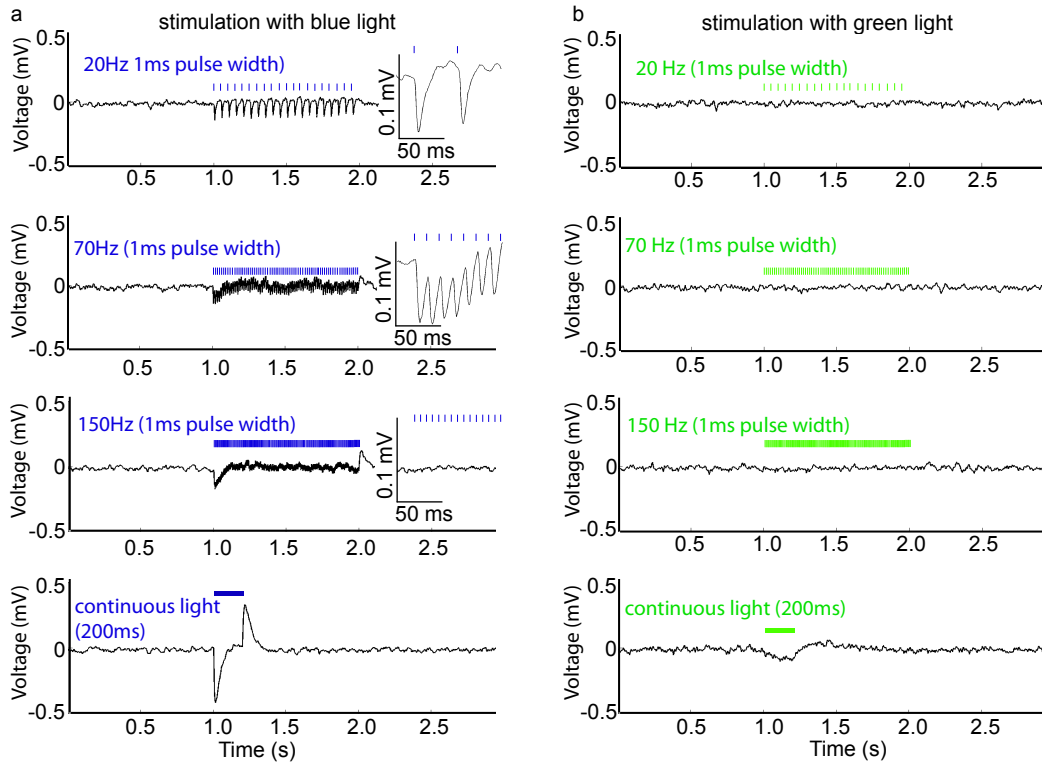


Supplementary Figure 6. Raster plots and PSTHs of neurons recorded at Chr2-expressing sites. **(a)** AAV5-hSyn-ChR2-EYFP and **(b)** AAV5-hThy-1-ChR2-EYFP. Boxes represent responses to 20, 50, 70, 150 Hz and continuous blue light stimulation. Blue ticks represent blue light stimulation. The pulse-triggered average is plotted with 1 ms resolution illustrating the latency of the excitation after the light pulse and light-evoked waveforms (blue) did not differ from spontaneous waveforms (black) (see insets).

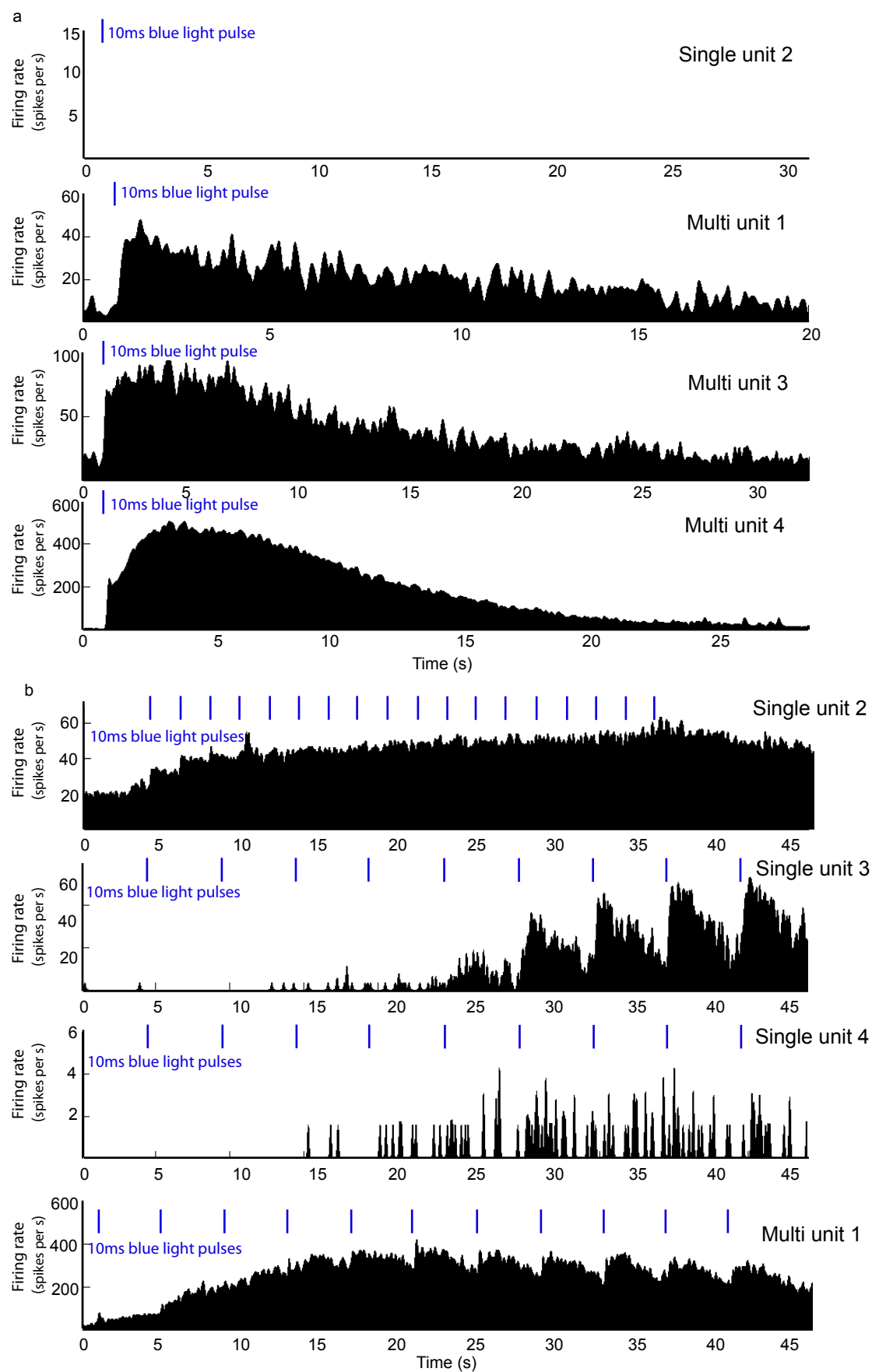


Supplementary Figure 7. Firing rate modulation of single and multi units recorded at ChR2 expressing sites. (a) AAV5-hSyn-ChR2-EYFP and (b) AAV5-hThy-1-ChR2-EYFP. Firing rates during stimulation are plotted against baseline firing rates (without stimulation). Empty circles show non-significant responses to light, filled circles show significant responses. Different colors represent different stimulation parameters (shown in separate panels): blue - 20Hz, magenta - 50 Hz, green - 70 Hz, violet - 150 Hz. Note that not all units were tested with the full set of frequencies. The dashed gray line is the unity-slope line, where baseline firing rate and stimulation firing rate are equal.

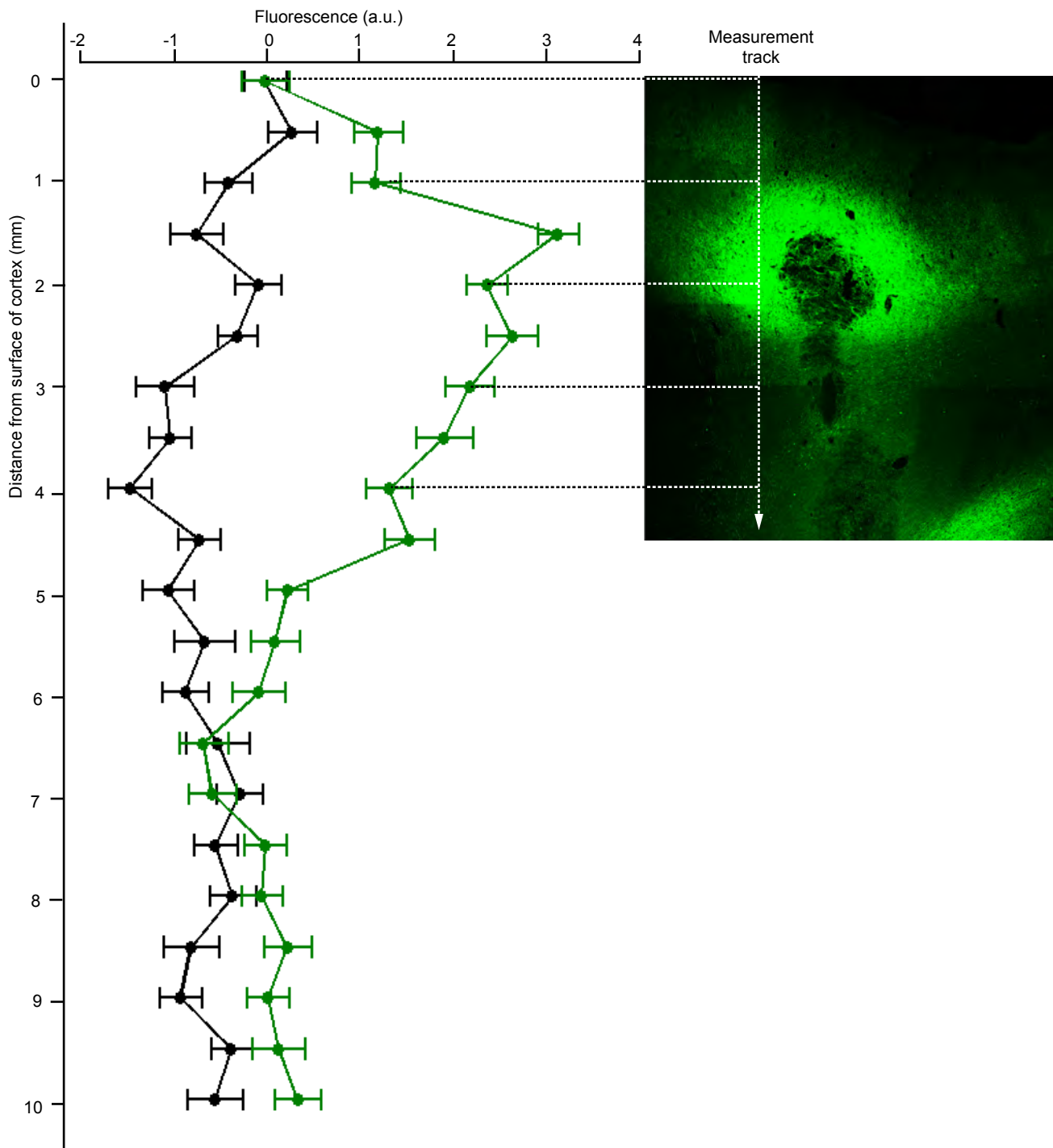
AAV5-hThy-1-ChR2-EYFP



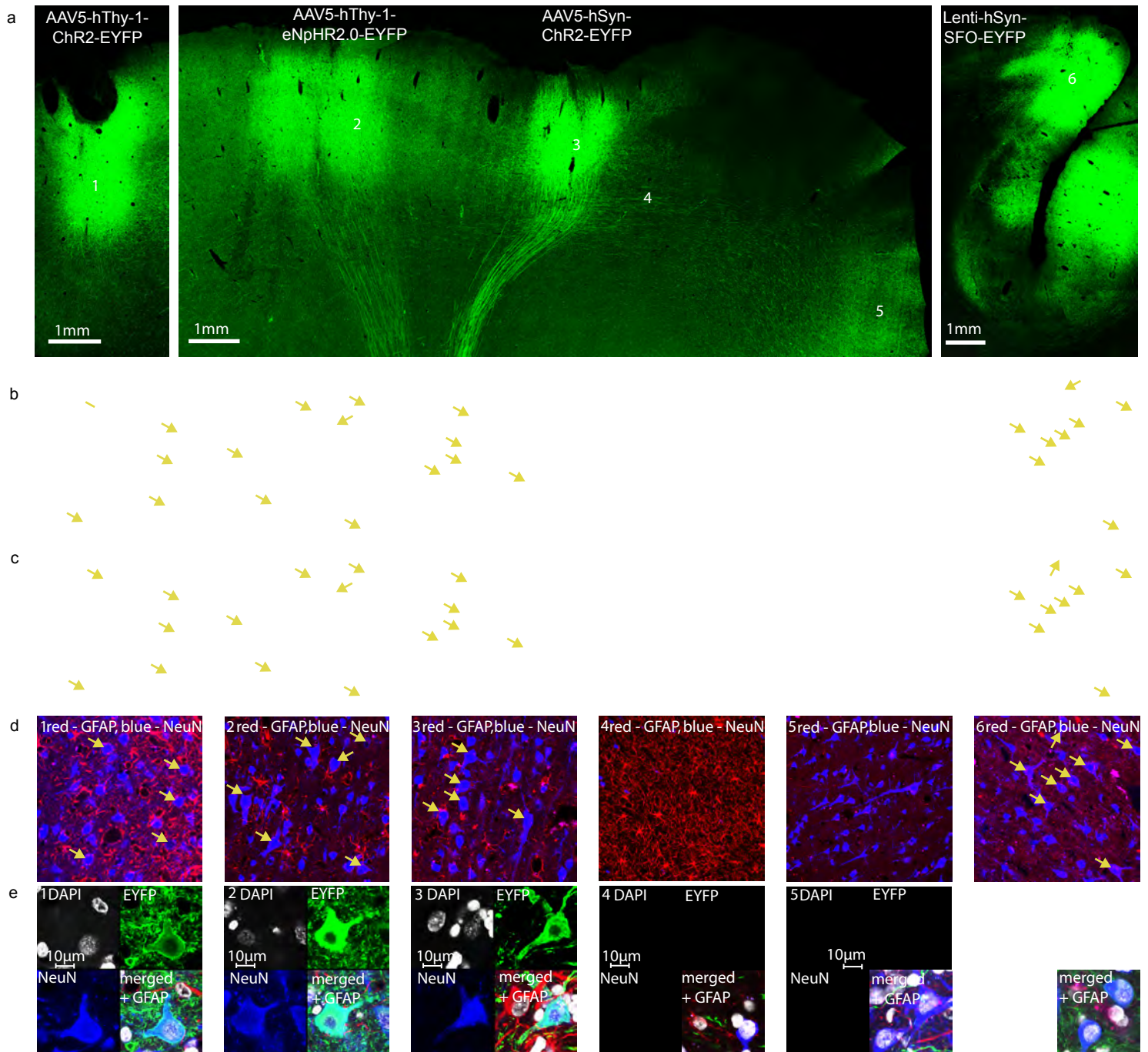
Supplementary Figure 8. Local field potential deflections in a ChR2-expressing regions during optical stimulation. **(a)** Local field potential deflections (averaged across 5 to 10 trials) in response to blue light with increasing frequencies from top to bottom (20, 70, 150 Hz and 200 ms continuous stimulation) at an AAV5-hThy-1-ChR2-EYFP injected site. Deflections are negative and show a positive rebound effect after the end of stimulation (particularly obvious for 200 ms continuous light). The deflections are in accordance with the expected ion flow: Na^+ flows into the cells when blue light is present causing a relative decrease of positive charges (negative deflections of the LFP signal) in the extracellular milieu. Insets depict an expanded view of the averaged LFP traces. **(b)** Measurements during green light stimulation at the same area as in a. No prominent LFP deflections are visible. Insets depict an expanded view of the averaged LFP traces.



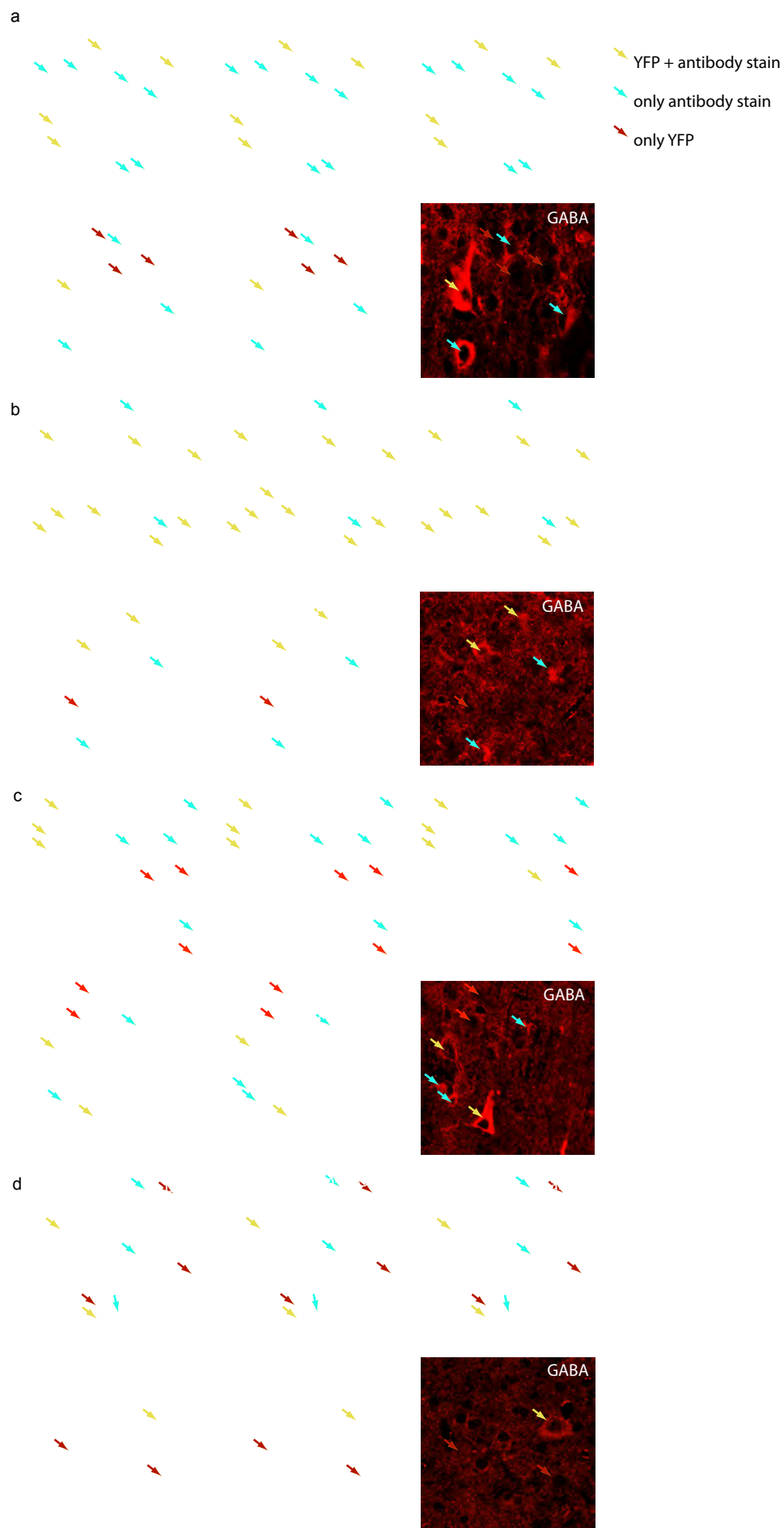
Supplementary Figure 9. Responses of single and multi units recorded at a SFO-EYFP expressing site. (a) Responses to a single 10 ms blue pulse. (b) Responses to a sequence of 10 ms blue pulses. We observed that two of those units responded only after 3 to 4 pulses demonstrating the accumulation of photons over multiple pulses. The putative mechanism for this is as follows: During the first light pulse, photons hit a subset of channels and open them. Since not all channels receive a photon this might not be sufficient to influence the spiking probability of a given neuron. Subsequent light pulses, however, deliver further photons that in a random fashion hit other channels and open them. Since SFO has a long lasting effect the channels opened during previous light pulses stay open. In this way the neuron eventually reaches an activation level that causes it to increase its spiking activity. This property of the SFO allows activations of large populations by a sequence of low light intensity pulses.



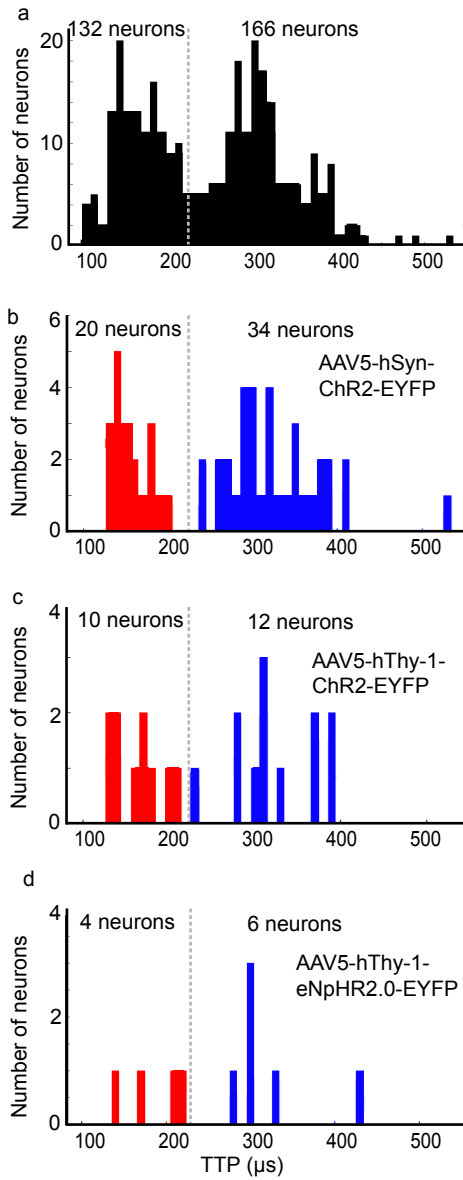
Supplementary Figure 10. Fluorescence measurements at injected and non-injected sites in the perfused brain. Image of injected and probed cortex (right) of monkey B and trace of fluorescence measurement (left, green curve, mean \pm SEM). The black curve represents measured values from visual cortex of the contralateral hemisphere (not injected with viral vectors and thus not expressing any fluorescent protein). Fluorescence intensities are plotted against penetration depth in cortex (distance between the surface of cortex and the tip of the fiber). The vertical dashed line indicates the measurement track and the horizontal dashed lines indicate depth of measurements in tissue. In contrast to quantified fluorescence at the injected site, there was no significant change measured in the control region of visual cortex. This confirms that fluorescence caused by the opsin-EYFP expression can be discriminated from auto-fluorescence in the primate brain.



Supplementary Figure 11. Staining of neuronal and astroglia cells. **(a)** Coronal slice through motor cortex injected with AAV5-hThy-1-ChR2-EYFP in monkey D (left panel), coronal slice through motor cortex injected with AAV5-hThy-1-eNpHR2.0-EYFP and hSyn-ChR2-EYFP, respectively, in monkey D (middle panel), and sagittal slice through area PE injected with Lenti-hSyn-SFO-EYFP in monkey B (right panel). Same figure as in main manuscript Fig. 5a. **(b)** Magnified views of the injected areas (indicated by numbers 1,2,3, and 6) and areas receiving projecting fibers (4 and 5). Arrows point out single EYFP-opsin expressing neurons. **(c)** Counter stain with the nuclear marker DAPI (white to gray). **(d)** Counter stain with the neuronal marker NeuN (blue), and the astroglia marker GFAP (red). **(e)** Close-up view of infected neurons (1, 2, 3 and 6) and projecting fibers (4 and 5). Positions are indicated by the same numbers as used in the overview images.



Supplementary Figure 12. Staining of inhibitory and excitatory neurons. (a) AAV5-hSyn-ChR2-EYFP, (b) AAV5-hThy-1-ChR2-EYFP, (c) AAV5-hThy-1-eNpHR2.0-EYFP, and (d) Lenti-hSyn-SFO-EYFP. Left panels illustrate nuclear stain (DAPI), middle panels show EYFP opsin expression, and right panels show antibody stain for CamKII (blue) and GABA (red). Yellow arrows point towards neurons which express EYFP and are colabelled by the respective antibody.



Supplementary Figure 13. Action potential waveform analysis. **(a)** Waveform width distribution measured as trough to peak (TTP) duration of waveforms of all recorded neurons. Gray dashed line represents 230 μs threshold between narrow and broad waveforms. **(b)** Waveform width distribution of significantly light responsive hSyn-ChR2 neurons (red, narrow waveforms; blue, broad waveforms). **(c)** Waveform width distribution of significantly light responsive hThy-1-ChR2 neurons. **(d)** Waveform width distribution of significantly light responsive hThy-1-eNpHR2.0 neurons.

construct	monkey	Single units responsive to light	Multi units responsive to light
AAV5-hSyn-ChR2	D	62/127 (50%)	54/87 (62%)
AAV5-hThy-1-ChR2	D	18/47 (38%)	12/20 (60%)
	B	6/6 (100%)	2/3 (67%)
AAV5-hThy-1-eNpHR2.0	D	55/144 (38%)	7/32 (22%)
Lenti-hSyn-SFO	B	4/12 (33%)	6/17 (26%)

Supplementary Table 1: Summary of significantly light responsive neurons ($p < 0.01$, $X^2 = 3.8415$, degrees of freedom = 1).

	AAV5-hSyn-ChR2-EYFP		AAV5-hThy-1-ChR2-EYFP		AAV5-hThy-1-eNpHR2.0-EYFP	
	significant cells (n = 62)	non-significant cells (n = 65)	significant cells (n = 18)	non-significant cells (n = 29)	significant cells (n = 55)	non-significant cells (n = 89)
Mean	4.0234	5.3087	12.8562	11.3054	4.5608	4.6565
Std	6.6148	7.5348	26.0445	11.4881	4.4108	5.8260
Min	0.0440	0.0484	0	0	0.01	0.01
Max	34.4812	41.2926	145.6960	38.2086	16.8303	28.9996
Median	1.1254	2.1942	6.5151	7.9051	2.8026	2.1686

Supplementary Table 2: Baseline firing rates of motor cortex neurons at opsin expressing sites.

Distance from cortical surface [μ m]	AAV5-hSyn-ChR2-EYFP middle of injection (YFP/NeuN)	AAV5-hSyn-ChR2-EYFP border of injection (YFP/NeuN)	AAV5-hSyn-ChR2-EYFP out of border (YFP/NeuN)	AAV5-hSyn-ChR2-EYFP 1.5mm away from border (YFP/NeuN)	AAV5-hSyn-ChR2-EYFP 10mm away from border (YFP/NeuN)
150	0/151 (0%)	2/245 (0.82%)	1/249 (0.4%)	0/228 (0%)	0/237 (0%)
450	10/132 (7.58%)	130/242 (53.72%)	3/185 (1.62%)	0/217 (0%)	0/170 (0%)
750	111/168 (66.07%)	154/199 (77.39%)	0/198 (0%)	0/163 (0%)	0/150 (0%)
1050	127/198 (64.14%)	188/246 (76.42%)	2/146 (1.37%)	0/177 (0%)	1/177 (0.56%)
1350	125/196 (63.78%)	140/202 (69.31%)	0/151 (0%)	0/115 (0%)	0/159 (0%)
1650	140/224 (62.5%)	32/165 (19.39%)	0/86 (0%)	0/45 (0%)	0/166 (0%)
1950	14/164 (8.54%)	1/141 (0.71%)	0/13 (0%)	0/24 (0%)	0/174 (0%)
total	527/1233(42.74%)	647/1440(44.93%)	6/1028 (0.58%)	0/960 (0%)	1/1233(0.08%)
	1174/2673 (43.92%)				

Supplementary Table 3: Efficiency of infection measured across cortical layers and at different distances from injection site (AAV5-hSyn-ChR2-EYFP). Number of neurons (visualized with a NeuN antibody stain - marker for all neurons) was compared to number of infected neurons (visualized by the fluorescent protein EYFP expressed by the neurons).

Distance from cortical surface [μm]	AAV5-hThy-1-ChR2-EYFP middle of injection (YFP/NeuN)	AAV5- hThy-1-ChR2-EYFP border of injection (YFP/NeuN)	AAV5- hThy-1-ChR2-EYFP out of border (YFP/NeuN)
150	0/151 (0%)	0/148 (0%)	2/207 (1%)
450	10/133 (7.51%)	6/288 (2.08%)	1/156 (0.64%)
750	113/175 (64.57%)	66/128 (51.56%)	0/109 (0%)
1050	136/219 (62.10%)	61/207 (29.47%)	0/111 (0%)
1350	135/227 (59.47%)	8/155 (5.16%)	0/113 (0%)
1650	111/191 (58.12%)	2/112 (1.79%)	0/120 (0%)
1950	162/239 (67.78%)	0/104 (0%)	0/96 (0%)
2250	56/160 (35%)	2/68 (2.94%)	0/100 (0%)
2550	2/196 (1.02%)	0/56 (0%)	0/108 (0%)
total	725/1691(42.87%)	145/1266(11.45%)	3/1120(0.27%)
	870/2957 (29.42%)		

Supplementary Table 4: Efficiency of infection measured across cortical layers and at different distances from center of injection site (AAV5-hThy-1-ChR2-EYFP). Number of neurons (visualized with a NeuN antibody stain -marker for all neurons) was compared to number of infected neurons (visualized by the fluorescent protein EYFP expressed by the neurons).

Distance from cortical surface [μm]	AAV5-hThy-1-eNpHR2.0-EYFP middle of injection (YFP/NeuN)	AAV5- hThy-1-eNpHR2.0 -EYFP border of injection (YFP/NeuN)	AAV5- hThy-1-eNpHR2.0 -EYFP out of border (YFP/NeuN)
150	0/173 (0%)	0/201 (0%)	0/217 (0%)
450	25/133 (18.80%)	2/191 (1.05%)	0/263 (0%)
750	90/143 (62.94%)	30/117 (25.64%)	2/139 (1.44%)
1050	64/160 (40.00%)	36/127 (28.35%)	10/161 (6.21%)
1350	95/147 (64.63%)	37/110 (33.64%)	15/145 (10.34%)
1650	85/151 (56.129%)	55/110 (50.00%)	22/179 (12.29%)
1950	63/121 (52.07%)	43/95 (45.26%)	17/175 (9.71%)
2250	17/60 (28.33%)	21/45 (46.67%)	17/109 (15.60%)
2550	9/33 (27.27%)	7/39 (17.95%)	1/65 (1.79%)
total	448/1121(39.96%)	231/1035(22.32%)	84/1453(5.78%)
	679/2156(31.49%)		

Supplementary Table 5: Efficiency of infection measured across cortical layers and at different distances from middle of injection site (AAV5-hThy-1-eNpHR2.0-EYFP). Number of neurons (visualized with a NeuN antibody stain -marker for all neurons) was compared to number of infected neurons (visualized by the fluorescent protein EYFP expressed by the neurons).

Distance from cortical surface [μ m]	Lenti-hSyn-SFO-EYFP middle of injection (YFP/NeuN)	Lenti-hSyn-SFO-EYFP border of injection (YFP/NeuN)	Lenti-hSyn-SFO-EYFP out of border (YFP/NeuN)
150	5/261 (1.92%)	10/293 (3.41%)	0/316 (0%)
450	86/282 (30.50%)	53/356 (14.89%)	2/250 (0.8%)
750	112/395 (28.35%)	42/322 (13.04%)	3/272 (1.10%)
1050	92/240 (38.33%)	10/123 (8.13%)	0/137 (0%)
1350	70/236 (29.66%)	0/53 (0%)	0/37 (0%)
1650	10/106 (9.43%)		
total	375/1520(24.67%)	115/1147(10.05%)	5/1012(0.49%)
	490/2667 (18.37%)		

Supplementary Table 6: Efficiency of infection measured across cortical layers and at different distances from middle of injection site (Lenti-hSyn-SFO-EYFP). Number of neurons (visualized with a NeuN antibody stain -marker for all neurons) was compared to number of infected neurons (visualized by the fluorescent protein EYFP expressed by the neurons).

	CamKII single stain	GABA single stain
AAV5-hSyn-ChR2	93/171 (54%)	22/153 (14%)
AAV5-hThy-1-ChR2	141/219 (64%)	36/105 (34%)
AAV5-hThy-1-eNpHR2.0	104/129 (81%)	24/115 (21%)
Lenti-hSyn-SFO	125/229 (55%)	31/111 (28%)

Supplementary Table 7: Inhibitory and excitatory neuron stain. Stains were performed on separate brain slices, so values may not add to 100 %.

construct	Broad spiking	Narrow spiking	Not classified
AAV5-hSyn-ChR2	34/54 (63%)	20/54 (37%)	8
AAV5-hThy-1-ChR2	12/22 (55%)	10/22 (45%)	2
AAV5-hThy-1-eNpHR2.0	6/10 (60%)	4/10 (40%)	45
Lenti-hSyn-SFO	1/4 (25%)	3/4 (75%)	0

Supplementary Table 8: Action potential waveform analysis. Classification of waveforms into broad (putative excitatory) and narrow (putative inhibitory) spiking neurons.

equipment	Specification/description	company	Catalogue number
optical fibers	Diameter 200 μm , NA 0.27 Patch Cord, Length: 3m, End A: FC/PC, End B: Flat Cleave, Furcation Tubing: FT030, (only 1" on FC/PC end))	Thorlabs (Newton, NJ)	BFL37-200-CUSTOM
electrodes	tungsten electrodes 78mm, 5-7M Ω at 1000Hz, 10 μA	FHC (Bowdoin, ME)	UEWLGCEEN1E
superglue	Krazy Glue Advanced Precision 5g	Krazy Glue (Columbus, OH)	TCL KG48348MR
blunt guide tubes	cut and smoothed 21G 1½ Needle	Becton, Dickinson and Company (Franklin Lakes, NJ)	305167
hand driven microdrive	Ruffner microdrive dual electrode	Crist Instrument Co Inc. (Hagerstown, MD)	3-NRMD-S2
grid	Short grid standard delrin, 19.5 mm tall	Crist Instrument Co Inc. (Hagerstown, MD)	6-YGD-D1A
Power meter	Compact Power and Energy Meter Console, Digital 4" LCD	Thorlabs (Newton, NJ)	PM100D
Power sensor	Slim Power Sensor, Si, 400 - 1100 nm, 500 mW	Thorlabs (Newton, NJ)	S130C C-Series
Blue laser	473 nm	Sanctity Laser Technology (Shanghai, China)	SVL-473-0100
Green laser	561 nm	CrystaLasers (Reno, NV)	CL-2000
Yellow laser	594 nm	Laserglow Technologies (Toronto, Ontario, Canada)	LRS-594-CFF-150-5
software for laser control	TEMPO Experiment Control System	Reflective Computing (Saint Louis, MO)	TEMPO Experiment Control System
pulse generator	Master-8 pulse generator	A.M.P.I. (Jerusalem, Israel)	Master-8
data acquisition system	Plexon data acquisition system:	Plexon (Dallas, TX)	
	recording software		RASPUTIN
	Plexon MAP system		MAP2001-036
	Preamplifier		PBX-077 2001
	Headstage		HST/8o50-G20
	8-channel (10-pin) Omentics		ADP/8o50-AMP-f-8

	.050-to-female amphenol pin adaptor		
Spike sorter	Plexon Offline Sorter	Plexon (Dallas, TX)	Plexon Offline Sorter Version 2.8.8

Supplementary Table 9: List of equipment for optical stimulation and neural recordings.

equipment	Specification/description	company	Catalogue number
Laser (Source 1) and laser driver	473nm	Laserglow Technologies (Toronto, Ontario, Canada)	LRS-0473-AFM
3 Fiber splitters	fiber optic 1 X 2 splitter, 200um core, 50/50 ratio, ruggedized package, FC connectors	Fiber Optic Network Tech. Co. (Surrey, British Columbia, Canada)	customized
2 connectors between laser/detector and fiber	FC/FC connectors	Thorlabs (Newton, NJ)	
Connector sleeves	FC/APC to FC/APC Mating Sleeves	Thorlabs (Newton, NJ)	ADAF3
DAQ system	Data Acquisition System	NI (National Instruments)	USB 6211
Filter wheel		Thorlabs (Newton, NJ)	(FW102B)
Photodetector (sensitive)	low-noise detector; Cooled Avalanche Photodiode	Hamamatsu (Hamamatsu City, Japan)	C4777-01 (APD)
Photodetector	Detector	Hamamatsu (Hamamatsu City, Japan)	C5460-01
Triple Output DC Power Supply	Power supply		BK Precision 1651A used at +5/G and +15/-15/G
DAQ card	Data acquisition card		NI USB 6211
Control software	LabVIEW	National Instruments Corp. (Austin, TX)	

Supplementary Table 10: List of components for in vivo fluorescence detector.